Conceptual Design of the Cooling System for 1700°C-class Hydrogen-Fueled Combustion Gas Turbines

**N. Kizuka, K. Sagae, S. Anzai,
S. Marushima, T. Ikeguchi and K. Kawaike**
Power Industrial Systems R&D Division
Hitachi Ltd., Ibaraki, 312-0034, Japan

ABSTRACT

The effects of three types of cooling systems on the calculated operating performances of a hydrogen-fueled thermal power plant with a 1,700°C-class gas turbine were studied with the goal of attaining a thermal efficiency of greater than 60%. The combination of a closed-circuit water cooling system for the nozzle blades and a steam cooling system for the rotor blades was found to be the most efficient, since it eliminated the penalties of a conventional open-circuit cooling system which ejects coolant into the main hot gas stream.

Based on the results, the water cooled first-stage nozzle blade and the steam cooled first-stage rotor blade were designed. The former features array of circular cooling holes close to the surface and uses a copper alloy taking advantage of recent coating technologies such as thermal barrier coatings (TBCs) and metal coatings to decrease the temperature and protect the blade core material. The later has cooling by serpentine cooling passages with V-shaped staggered turbulence promoter ribs which intensify the internal cooling.

INTRODUCTION

Energy consumption continues to rise with industrial growth, though it has been a long time since the conservation of natural energy resources was first advocated. Environmental pollution, caused by industrial development, has become serious worldwide. To mitigate these energy and environmental problems, the Japanese government has instituted the International Clean Energy Network Using Hydrogen Conversion (WE-NET) Program, a 28-year effort from 1993 to 2020. The studies have been administrated through the New Energy and Industrial Technology Development Organization (NEDO) as a part of the WE-NET program with funding from the Agency of Industrial Science and Technology (AIST) in Ministry of International Trade and Industry (MITI) of Japan. This research and development work in above-mentioned program has been directly entrusted by the Japan Power Engineering and Inspection Corporation (JAPEIC).

The final objective is to achieve an ecologically clean and an efficient hydrogen-fueled energy-conversion system. The combustion of pure hydrogen with pure oxygen produces only steam; it does not emit CO_2, NOx, or SOx. The goal is achieving a thermal plant with an efficiency of greater than 60% high heating value (HHV) or 71% low heating value (LHV) at a turbine inlet temperature of 1,700°C, to compensate energy losses that occur during production, transportation, and storage of valuable hydrogen. Hitachi is taking part in research and development program to develop an effective cooling system for hydrogen-fueled combustion gas turbines. The performance of such a high temperature turbine depends greatly on the coolant consumption, thus one of the keys is an effective cooling scheme for turbine blades including a cooling system, selection of coolant and a cooling circuit.

It has been indicated that closed-circuit cooling systems for a current Brayton cycle gas turbine are effective to achieve higher thermal efficiencies by suppressing compressor work used to supply coolant to blades, dilution of the hot gas temperature with the coolant, aerodynamic mixing loss, and rotor blade pumping loss and by effective recovery of heat exchanged coolant (Kawaike, et al. 1984; Alderson, et al., 1987; Ikeguchi, et al., 1994). Thus the authors intended to apply the same methodology, the closed-circuit cooling systems, to a hydrogen-fueled thermal power plant.

In addition, water cooling was considered for the stationary nozzle blades, which is superior to steam cooling as a cooling medium. As for the moving rotor blades, closed-circuit internal steam cooling was chosen to avoid the expectable problems such as water leakage and difficulty in recovering water through the turbine rotor. The idea of water cooling was tried and tested for both nozzle and rotor blades featuring a composite material construction under high temperature turbine technology (HTTT) program (Geiling, et al., 1983), though water cooled gas turbines have not been in practical use until now.

This paper will firstly discuss the studied effect of the cooling system on a plant performance based on the H_2/O_2 Fired High Temperature Steam Cycle (HTSC) (Jericha, et al., 1991). Following
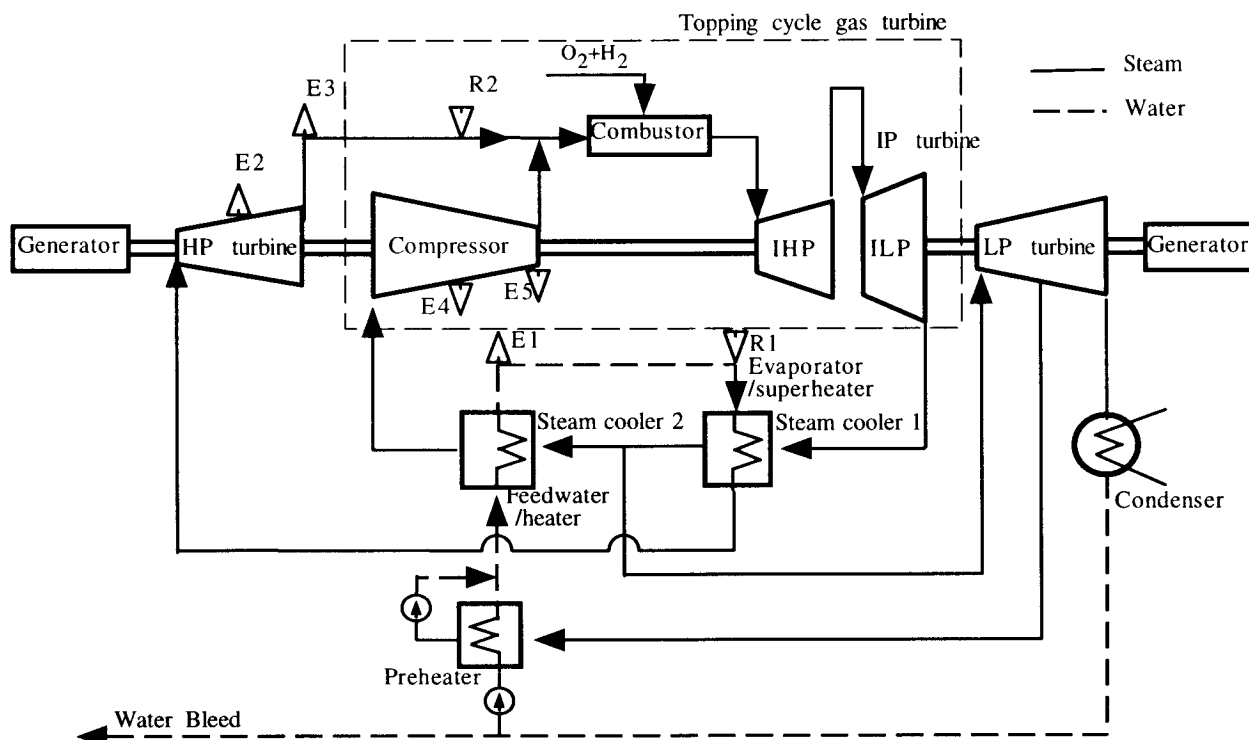
Figure 1. Components of HTSC plant

Table 1. Main component parameters

IP Turbine (Topping Cycle Gas Turbine)	
Compressor	
Inlet pressure (MPa)	0.14
Inlet temperature (℃)	114
Outlet pressure (MPa)	4.90
Rotational speed (rpm)	6,500
Combustor	
Fuel	$H_2 + O_2$
Outlet temperature (℃)	1,700
Turbine	
Stage	2(IHP)+6(ILP)
Rotational speed (rpm)	6,500(IHP), 3,000(ILP)
Inlet gas flow (kg/s)	222.3
Outlet pressure (MPa)	0.16
Bottoming Cycle	
HP Turbine	
Inlet pressure (MPa)	19.00
Outlet pressure (MPa)	5.00
LP Turbine	
Inlet pressure (MPa)	0.15
Outlet pressure (MPa)	0.05

the result that the closed-circuit cooling system was essential to achieve a targeted thermal efficiency of 60% HHV, the conceptually designed cooling circuit and the cooled first-stage nozzle and rotor blades will be presented. Attention is paid not only to enhance cooling but also to reduce large thermal gradients across the blade materials by taking advantage of recent coating technologies.
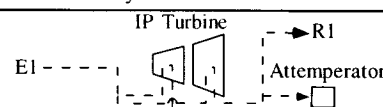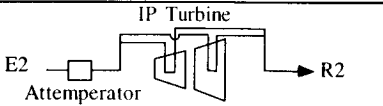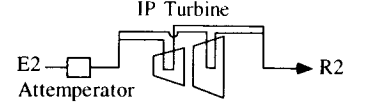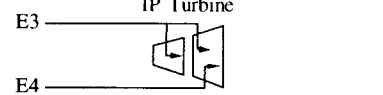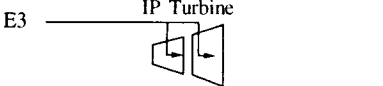
EFFECT OF COOLING SYSTEM

The HTSC, shown in Fig.1, has two closed cycles: the topping and bottoming cycles. The former consists of a compressor, combustor, intermediate pressure (IP) turbine, steam cooler 1, and steam cooler 2. The later consists of low pressure (LP) turbine, condenser, preheater, high pressure (HP) turbine, combustor, and IP turbine. The combination of the compressor, combustor and twin-shaft IP turbine corresponds to a topping cycle gas turbine. The twin-shaft IP turbine has intermediate high pressure (IHP) and intermediate low pressure (ILP) turbines.

The main component parameters used to analyze the cycle performance are shown in Table 1. The key points to achieve a high efficiency are to increase the outlet temperature of the IP turbine to generate more steam in the bottoming cycle and to increase the inlet temperature of the LP turbine to obtain more power. To meet them and cope with the high temperature of the IP turbine inlet, three types of cooling systems were selected and their effects were investigated. The three are:

(1) closed-circuit water cooling system for nozzle blades and steam cooling system for rotor blades (CCWCN-SCR);

(2) closed-circuit steam cooling system for nozzle and rotor blades (CCSCN-R); and

(3) open-circuit steam cooling system for nozzle and rotor blades

Table 2. Supply and recovery points of coolants

Cooling System	Blade	Supply		Recovery		System
(1) Closed-circuit water for nozzle blades and steam cooling system for rotor blades (CCWCN-SCR)	Nozzle	Feedwater /heater	E1	Evaporator /superheater	R1	IP Turbine — R1, Attemperator (E1 - - - -)
	Rotor	HP Turbine Middle Stage	E2	Combustor Inlet	R2	IP Turbine, E2 → Attemperator → R2
(2) Closed-circuit steam cooling system for nozzle and rotor blades (CCSCN-R)	Nozzle & Rotor	HP Turbine Middle Stage	E2	Combustor Inlet	R2	IP Turbine, E2 → Attemperator → R2
(3) Open-circuit steam cooling system for nozzle and rotor blades (OCSCN-R)	Nozzle	HP Turbine Outlet / Compressor Middle Stage	E3 / E4	———	—	IP Turbine, E3, E4
	Rotor	Compressor Middle Stage	E3	———	—	IP Turbine, E3

(OCSCN-R).

In this analysis inlet gas flow of the IP turbine was fixed constant to achieve a plant power output of about 500 MW, and inlet and outlet pressures of HP and LP turbines were also kept constant. In each cooling system, coolants are supplied from and recovered at the points of the cycle as shown in Fig.1 and Table 2.

(1) CCWCN-SCR system

Nozzle blades are cooled with 100℃ water supplied from the feedwater heater (E1). After cooling, the heat exchanged water is returned to the evaporator/superheater (R1) and part of it is supplied to the attemperator to cool steam for cooling the rotor blades. Rotor blades are cooled with steam that is extracted from the middle stage of the HP turbine (E2) and cooled in the attemperator to 300℃. After cooling, the heat exchanged steam is returned to the combustor inlet (R2). The thermal energy gained by closed-circuit cooling is recovered at the evaporator and combustor. Interstage sealing steam for the IHP turbine is extracted from the compressor outlet (E5), while more interstage sealing steam for the ILP turbine is extracted from the middle stage of the compressor (E4). Interstage sealing steam for both the IHP and ILP turbines is finally ejected into the main stream gas.

(2) CCSCN-R system

Nozzle and rotor blades are cooled with steam that is extracted from the middle stage of the HP turbine (E2) and cooled by the attemperator to 300℃. After cooling, the heat exchanged steam is returned to the combustor inlet (R2). The thermal energy gained by closed-circuit cooling is recovered at the combustor. Interstage sealing steam for the IP turbine is extracted as well as that of system (1) and finally ejected into the main stream gas.

(3) OCSCN-R system

Cooling and interstage sealing steam of 385℃ is extracted from the HP turbine outlet (E3) for all blades of the IHP turbine, and the fore two stage nozzle and all rotor blades of the ILP turbine. More cooling and sealing steam of 362℃ is extracted from the middle stage of the compressor for the rest of the nozzle blades of the ILP turbine. The spent steam is finally discharged into the main stream gas.

Evaluation

The analyzed cycle performance results based on cooling systems (1), (2) and (3) are shown in Table 3 in comparison with the performance of a no cooling system as an ideal case. System (1) was found to be the most efficient. The relative decreases in the plant efficiencies between the no cooling system and systems (1) and (2) were 2.0% and 4.2%. However the efficiency of system (3) decreased by 10.4% despite its total cooling steam flow ratio being almost the same as that of system (1) and two-thirds of that of system (2). This was because system (3) had an open-circuit cooling steam flow ratio of 27.9%, which was about five times as much as the values of systems (1) and (2), and this decreased the outlet temperature of the IP turbine to 673℃ about 130℃ lower than in systems (1) and (2), caused by dilution of main stream gas with the coolant. The decrease in the IP turbine outlet temperature reduced the amount of steam generated in the bottoming cycle, in other words the amount of steam returned to the LP turbine inlet decreased and the amount of steam returned to the compressor inlet increased instead, so that the compressor work increased and the efficiency decreased. However, the decrease in the IP turbine outlet temperatures of systems (1) and (2) were held within 70℃, so the high efficiencies were obtained. This means that open-circuit cooling system is not effective for the HTSC.

Comparison of systems (2) to (1) showed that system (2)

required the amount of closed-circuit cooling steam which was twice as much as that of system (1) from the middle stage of the HP turbine and double the amount of spent steam was returned to the combustor inlet. That decreased the HP turbine output by 9.0MW and increased the compressor work by 4.1MW. However in system (1) the cooling water was returned to the evaporator/superheater (R1) and supplied to the HP turbine inlet, so it could achieve performances closer to those of the ideal no cooling system. Therefore system (1) had an efficiency of 60.1%, which were closer to 61.3% of the no cooling system, meeting the target.

Table 3. Performance results

Cooling System		No Cooling (base)	(1) CCWCN -SCR	(2) CCSC N-R	(3) OCSC N-R
Plant efficiency	(HHV%)	61.3	60.1	58.7	54.9
Plant output	(MW)	497	513	508	458
IP turbine output	(MW)	488	485	488	509
HP turbine output	(MW)	43.2	44.0	35.0	35.6
LP turbine output	(MW)	78.3	77.2	82.1	73.2
Compressor work	(MW)	99.0	78.9	83.0	147
Mechanical loss	(MW)	13.6	14.3	13.7	12.7
Open-circuit cooling steam flow ratio	(%)	-	5.5	5.7	27.9
Closed-circuit cooling steam flow ratio	(%)	-	19.7	40.8	-
Total cooling steam flow ratio	(%)	-	26.2	46.5	27.9
IP turbine outlet temperature (℃)		866	798	806	673

COOLING CIRCUIT OF GAS TURBINE

The gas path and cooling circuits of the compressor, combustor and IP turbine based on cooling system (1) were conceptually designed as shown in Fig. 2. The HP turbine, compressor and IHP turbine are operated at the rotational speed of 6,500 rpm and the ILP and LP turbines are operated at 3,000 rpm. The compressor has 20 stages with a 4.90 to 0.14 pressure ratio and the axial length is approximately 1,800 mm. The axial length of the IP turbine is approximately 3,300 mm which includes the shaft bearing space from which cooling steam is supplied between the second and third stages.

Water for cooling the nozzle blades is externally supplied from the bottoming cycle through the outer casing and the heat exchanged water is returned to the bottoming cycle. Steam for cooling rotor blades of the IHP turbine is externally supplied from the bottoming cycle into the rotor shaft end through the outer casing and it flows through the inner paths of the rotor disks to each rotor blade. After cooling the blades the heat exchanged steam returns to another inner paths of the rotor disks until it finally reaches the combustor inlet. More steam for cooling rotor blades of the ILP turbine is externally supplied into the rotor shaft end as well. After cooling the blades the heat exchanged steam is collected to the other rotor shaft end and returned to the casing outside. The steam is finally combined with discharged steam from the bottoming cycle in the combustor inlet.

DESIGN OF COOLED BLADES

The cooling configuration of the water cooled first-stage nozzle and the steam cooled first-stage rotor blade needed to apply closed-circuit cooling system (1) were designed.

Nozzle Blade

The cooling design concepts for the first-stage nozzle blade (Fig. 3) were;
(1) having a blunt leading edge to reduce the thermal load at the leading edge region;
(2) applying a copper alloy, whose thermal conductivity is about 15 times greater than that of conventional nickel base alloys, to reduce the metal temperature and thermal stress;
(3) allocating many circular cooling holes as close to the blade surface as possible to keep the temperature below the allowable temperature of copper alloy of about 400℃;
(4) having water cooling of outer and inner endwalls by drilled cooling passages; and
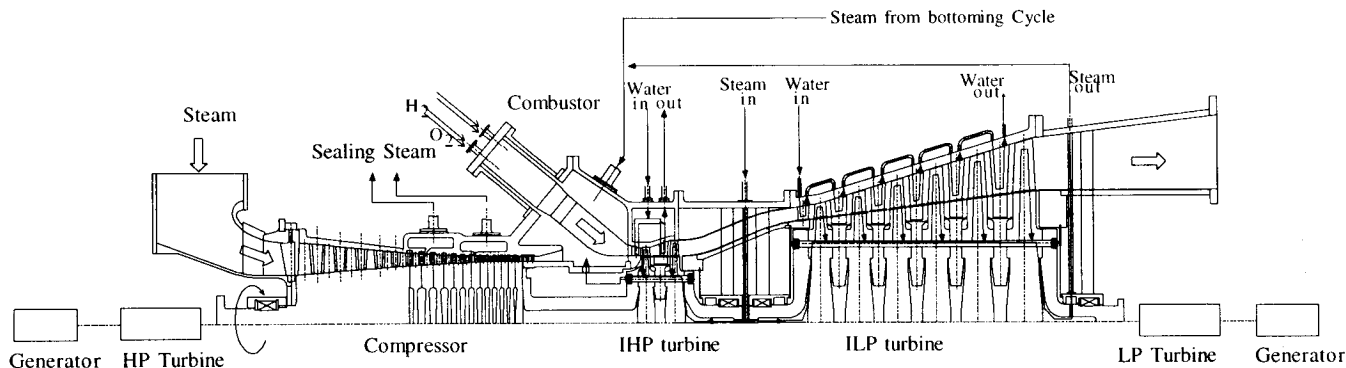(5) having a thermal barrier coating (TBC) to reduce the thermal-load and protect the metal surface.

Figure 2.   Schematic view of gas path and cooling circuits of gas turbine
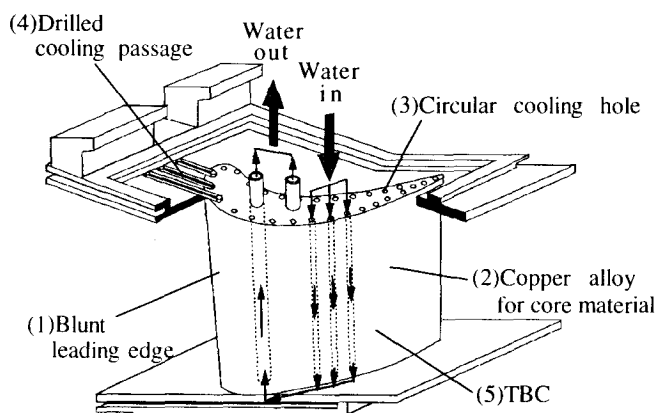
Figure 3. The first-stage nozzle blade design concepts

Before designing the cooled blade, three copper alloys were selected for the blade core material with respect to high allowable temperature and toughness:
(1) copper alloy containing Cr and Zr (CZ-Cu);
(2) copper alloy containing Ni, Si, and Zr (NSZ-Cu); and
(3) oxide dispersion strengthened copper (ODS-Cu).

The examined mechanical properties of CZ-Cu, NSZ-Cu, and ODS-Cu at 300°C are shown in Table 4. The thermal conductivity of NSZ-Cu was about 30% lower than that of CZ-Cu and ODS-Cu, while ODS-Cu was inferior to CZ-Cu and NSZ-Cu in 0.2% yield and tensile strength. Therefore CZ-Cu was chosen for the water cooled first-stage nozzle blade.

Table 4. Mechanical properties of copper alloys at 300°C

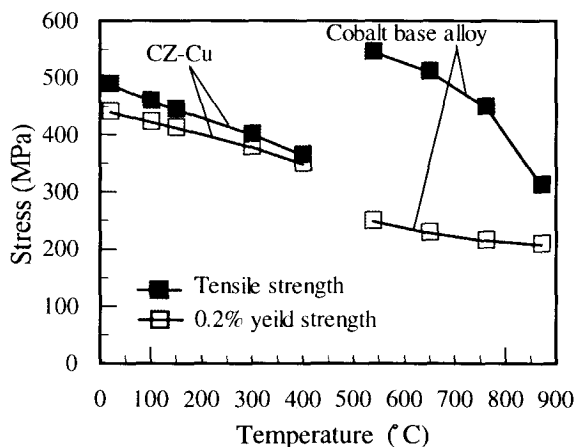|		CZ-Cu	NSZ-Cu	ODS-Cu
Thermal conductivity	(W/mK)	331	246	332
0.2% yield strength	(MPa)	375	379	255
Tensile strength	(MPa)	395	422	267
1000h creep rupture strength	(MPa)	333	127	69

Figure 4. Comparison of tensile and 0.2% yield strength

The tensile and 0.2% yield strength of CZ-Cu are compared with those of a typical cobalt base alloy, which has been used for nozzle blades, in Fig. 4. It was found that CZ-Cu had the appropriate strength as well as the cobalt base alloy as long as it was used under 400°C. As regards low cycle fatigue, detailed research is necessary, because any cracks are not allowed for water cooled nozzle blades.

Thermal stresses of three combinations of copper alloy and coatings were compared by analyzing the two-dimensional heat conduction model (Fig. 5). The three were:
(a) the copper alloy with no coating;
(b) the copper alloy coated with Inconel[1] 600 alloy (IN-600); and
(c) the copper alloy coated with a TBC.

As regards case (b), IN-600 was applied mainly because of corrosion resistance and partly because of thermal barrier effect. As regards case (c), a TBC was used to decrease the temperature of the copper alloy because of its lower thermal conductivity compared with metal. The total thicknesses of the TBC including its bond layer of 0.1 mm and IN-600 were 0.3 mm.
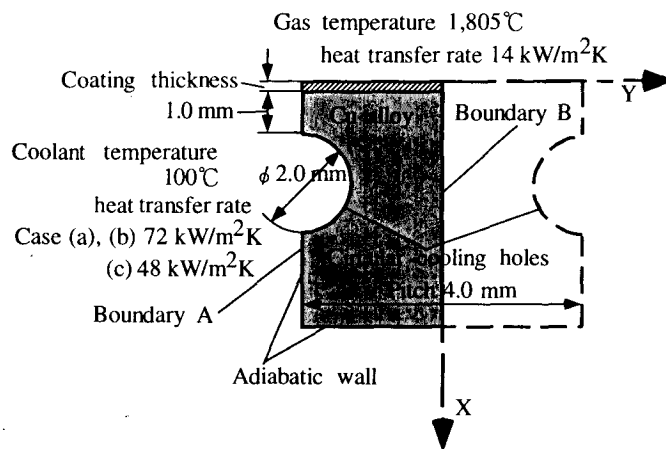

Figure 5. Two-dimensional heat conduction model

Design conditions were determined taking the thermally hardest section of the blade into account. Two kinds of coolant heat transfer rates were assumed to keep the copper alloy below the allowable temperature of 400°C as shown in Fig. 5. As to cases (a) and (b), the heat transfer rate of 72 kW/m²K was required by using the coolant velocity of 10 m/s above the usual maximum usage of 6 m/s, while as to case (c), the heat transfer rate of 48 kW/m²K provided by the velocity of 6 m/s was sufficient. The allowable limit of thermal stress was assumed at 360 MPa, which was the tensile strength at 400°C.

The model had a symmetrical shape, so only one side was solved. Thermal deformation along the Y-direction with boundaries A and B staying parallel to each other was assumed to be free. The temperature and thermal stress distributions along the X-direction are shown in Fig. 6. The maximum temperature of the copper alloy of cases (a), (b) and (c) were 393, 353 and 244°C, respectively. The maximum thermal stresses of the copper alloy of cases (a), (b), and

---

[1] Trademark of Inco Alloys International, Inc.

(c) were 340, 250, and 124 MPa, respectively. Case (a) has no margin. Coatings are thought to be necessary not only to decrease the temperature and to reduce the thermal stress but also to protect surface of the copper alloy from corrosion. Comparison of cases (b) to (c) indicates that (b) requires the greater coolant velocity to achieve the greater coolant heat transfer to meet the design limit due to the weaker thermal barrier effect of the IN-600, while case (c) mostly depends on the thermal barrier effect of the TBC. Although both thermal gradients of the coating of cases (b) and (c) are greater than current level, it should be noted that the allowable strength of the TBC is much less than that of the IN-600. With respect to toughness and durability of the coating, case (b) is thought to be probable, however the required coolant velocity is high. In this case water erosion problem is necessary to be examined, or use of another metal coating that has lower heat conductivity is conceivable to reduce the velocity. On the other hand, with respect to the thermal barrier effect, case (c) is thought to be probable, however the reliability and durability of the coating are currently low. The verification tests are needed under such thermal load conditions and they are underway.
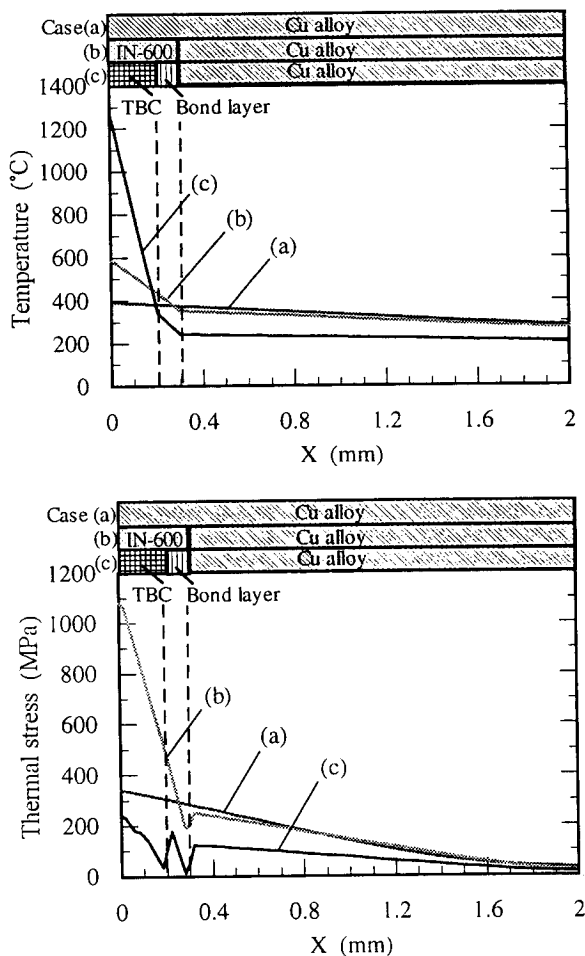
The design conditions for the nozzle blade are shown in Table 5. The peak temperature distribution factor at the inlet of the first-stage nozzle blade was assumed to be 10%. Since CZ-Cu has an allowable temperature of 400°C, the cooling effectiveness of 83% was required. The cooling effectiveness is defined as,

$$\text{Cooling effectiveness} = \frac{\text{gas temp. - blade metal temp.}}{\text{gas temp. - coolant supply temp.}}$$

Table 5. Design conditions of nozzle blade

Blade inlet average total temperature	(°C)	1,700
inlet peak total temperature	(°C)	1,805
inlet total pressure	(MPa)	4.66
exit static pressure	(MPa)	3.65
Cooling water inlet temperature	(°C)	100
inlet pressure	(MPa)	9.81
outlet pressure	(MPa)	8.83

Figure 7 shows the calculated temperature distribution of the blade mean section. The water cooled nozzle blade designed here had a two layers TBC with a total thickness of 0.3mm. It had a one-circuit, 62-passage multihole cooling design. The diameter of the circular holes and the pitch were 2.0 and 4.0 mm, respectively.

Although the trailing edge section had to be cooled by only an array of cooling holes, the maximum temperature was 313°C, meeting the allowable limit. The surface average cooling effectiveness of 91% was obtained at the cooling flow ratio of 16.3%. The heat flux passing through the TBC was about 7.4 MW/m^2.
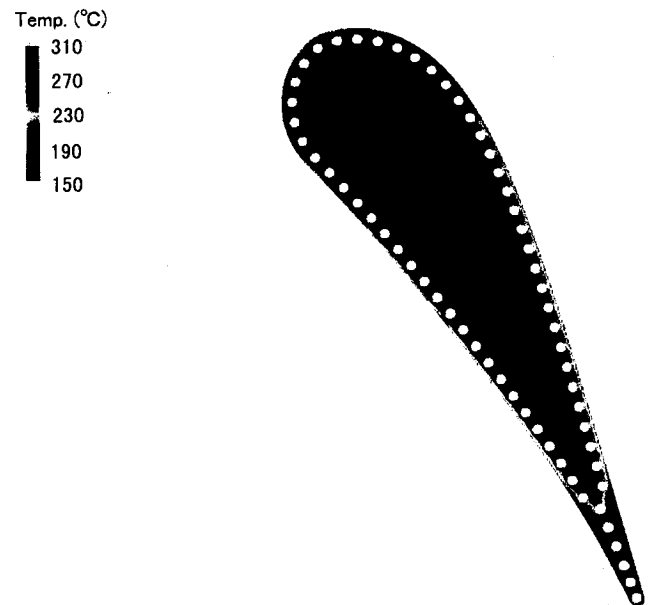
Figure 6. Temperature and thermal stress distributions

Figure 7. Calculated temperature distribution

Rotor Blade

As mentioned, water cooling was thought to be difficult to be applied to the rotor blades which were moving parts, because of difficulties in recovering water, preventing leakage, and configuring

complicated cooling paths in the rotor shaft, despite its superior thermal properties as a coolant. Thus, to achieve closed-circuit cooling with steam for the rotor blades, intensified internal cooling techniques were required.

The cooling design concepts for the first-stage rotor blade (Fig. 8) were:

(1) having a blunt leading edge to reduce thermal load at the leading edge region as well as the nozzle blade;

(2) applying V-shaped staggered turbulence promoter ribs (Anzai, et al., 1991; Kawaike, et al., 1993) in the serpentine cooling passage to enhance internal heat transfer;

(3) minimally allocating film cooling holes at only the leading edge region to achieve closed-circuit cooling as much as possible; and

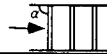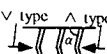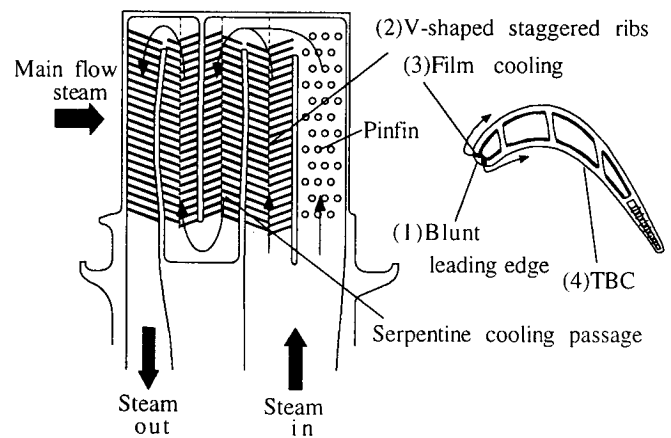(4) having a TBC to reduce the thermal load and protect the metal surface.

Figure 8. The first-stage rotor blade design concepts

As to turbulence promoter ribs, Table 6 summarizes some of the relevant studies on heat transfer enhancement. Among these studies, V-shaped staggered ribs have been the most efficient, though the experimental methods and conditions were different.

Table 6. Summary of relevant studies on heat transfer enhancement of turbulence promoter ribs

f : Pressure loss coefficient,   Nu : Nusselt number
P/e : Pitch / Rib height,   Re : Reynolds number
α : rib angle,   suffix s : smooth duct

| Rib configuration	Author(s)	Rib parameters Shape, α, P/e		Nu/Nu_s	f/f_s	$\dfrac{Nu/Nu_s}{(f/f_s)^{1/3}}$
Transverse ribs	Han et al., 1985	, 90°, 10		2.1 - 2.5	5.8 - 6.8	1.2 - 1.3
	Kukreja et al., 1991			2.4 - 2.6	4.8 - 6.5	1.4
	Anzai et al. 1991			2.4 - 2.7	4.9 - 6.0	1.4 - 1.5
	Taslim et al., 1994			2.2 - 2.4	10 - 13	1.0
Angled rib	Han et al., 1985	, 75°, 10		3.3	5.3 - 9.5	1.6 - 1.9
		, 60°, 10		2.5 - 3.2	7.2 - 10	1.4 - 1.5
		, 45°, 10		2.9-3.0	4.3 - 6.4	1.6 - 1.7
	Anzai et al., 1991	, 70°, 10		3.2 - 3.5	6.5 - 8.5	1.7
	Taslim et al., 1994	, 45°, 10		3.1 - 3.8	11 - 14	1.4 - 1.6
V/∧ shaped ribs	Han et al., 1985	V, 60°, 10		2.8 - 3.6	8.0 - 11	1.4 - 1.6
		V, 45°, 10		2.5 - 3.3	8.0 - 10	1.3 - 1.5
		∧, 60°, 10		2.4 - 3.3	8.5 - 13	1.2 - 1.4
		∧, 45°, 10		2.3 - 3.0	8.0 - 11	1.2 - 1.4
	Anzai et al., 1991	V, 70°, 10		2.7 - 4.3	8.0 - 11	1.4 - 1.9
		∧, 70°, 10		2.7 - 3.9	8.0 - 9.3	1.4 - 1.9
	Taslim et al., 1994	V, 45°, 10		2.9 - 3.3	13 - 17	1.7
Transverse staggered ribs	Kukreja et al., 1991	(a)	90°, 10	3.4 - 3.8	7.5 - 11	1.7
			90°, 20	2.6 - 2.8	4.0 - 6.5	1.5 - 1.6
		(b)	90°, 20	3.3 - 3.5	6.5 - 10	1.5 - 1.8
			90°, 20	1.3 - 1.6	4.0 - 6.0	1.3 - 1.5
		(c)	90°, 20	3.0 - 3.2	5.1 - 6.5	1.4 - 1.8
	Anzai et al., 1991	(a)	90°, 5	4.6 - 5.8	18 - 19	1.8 - 2.2
			90°, 10	3.2 - 3.9	6.5 - 10	1.7 - 1.8
V/∧ staggered ribs	Anzai et al., 1991	V, 70°, 5		5.9 - 6.6	10 - 13	2.7 - 2.8
		V, 70°, 10		3.0 - 5.0	10 - 11	1.4 - 2.2
		∧, 70°, 5		3.5 - 4.1	7.4 - 8.0	1.8 - 2.1
		∧, 70°, 10		2.5 - 3.1	5.0 - 6.0	1.5 - 1.7
	Taslim et al., 1994	∧, 45°, 10		2.7 - 3.0	8.3 - 10	1.3 - 1.4
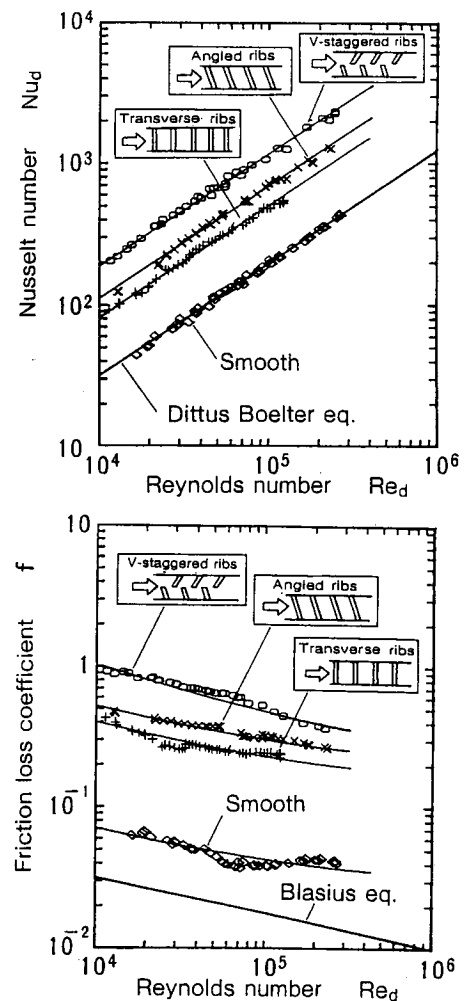
Figure 9. Heat transfer and pressure loss characteristics

Figure 9 shows the comparison of heat transfer and pressure loss characteristics of typical turbulence promoter ribs conducted by the authors using the same experimental apparatus and measuring method. The heat transfer rate of V-shaped staggered ribs (Angle=20 degree, pitch/ rib height=5) improved 2.4 times greater than that of transverse ribs and 1.7 times greater than that of angled ribs without much increase of pressure loss.

The design conditions for the rotor blade are shown in Table 7. The radial temperature distribution factor at the inlet of the first-stage rotor blade was assumed to be 6%. Single crystal (SC) alloy with an allowable temperature of 950℃ was selected for the material and two layers TBC of the total thickness with 0.3 mm was applied. The cooling configurations, i.e. cooling passages, film cooling holes and turbulence promoter ribs were determined by using the integrated CAE system for a cooled turbine blade (Kawaike, et al., 1992). The steam cooled rotor blade had a one-circuit, five-passage serpentine cooling design.
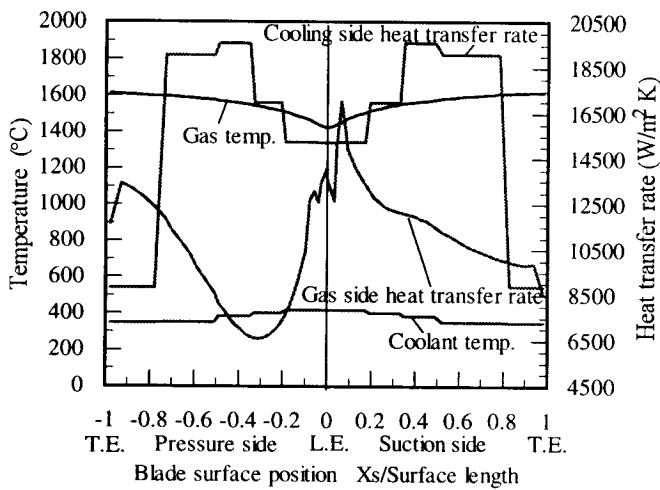

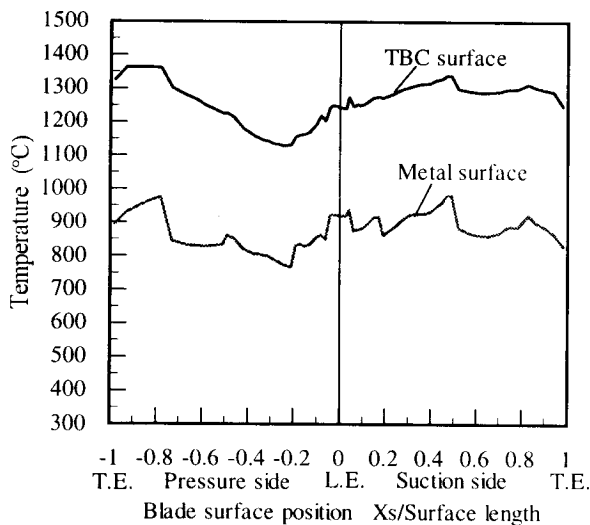**Figure 10.   Thermal conditions of rotor blade**

Figure 11.   Temperature distributions of rotor blade

Table 7.   Design conditions of rotor blade

Blade inlet average relative total temperature	(℃)	1,622
inlet peak relative total temperature	(℃)	1,699
inlet relative total pressure	(MPa)	3.69
exit static pressure	(MPa)	3.01
Cooling steam inlet temperature	(℃)	300
inlet pressure	(MPa)	5.88
outlet pressure	(MPa)	4.71

The thermal conditions and calculated temperature distributions of the blade mean section are shown in Figs.10 and 11. The main stream gas of steam increased the heat transfer rate up to 16.5 kW/m^{2}K at the leading edge section (Fig.10) and that required film cooling. The metal surface temperature was almost entirely kept within 950℃ because of the intensified internal cooling at the total cooling flow ratio of 5.0% (Fig. 11). The open-circuit cooling flow ratio for the film cooling and closed-circuit cooling flow ratio were 2.3% and 2.7%, respectively. The surface average cooling effectiveness of 58.5% was obtained. However, the maximum TBC surface temperature reached 1350℃ and the TBC had a maximum thermal gradient of 400℃ in 0.2 mm. The maximum heat flux passing through the TBC was 3.6 MW/m^2. These are about three times as much as current usage. Although this design entirely depends on the TBC severely requiring its reliability and durability and exceeds current level, the development of such coatings are thought to be within the scope in the near future.

CONCLUSION

The performances of a thermal plant having three different types of cooling systems for a 1,700℃-class hydrogen-fueled combustion gas turbine were analyzed. The results indicated closed-circuit cooling systems were more effective for achieving high efficiencies than conventional open-circuit cooling systems. This was because the closed-circuit cooling systems can eliminate penalties of conventional open-circuit cooling systems such as dilution of main stream gas with the coolant, mixing loss, and pumping loss. Furthermore, it was found that the closed-circuit water cooling system for nozzle blades and steam cooling system for rotor blades (CCWCN-SCR) exceeded the closed-circuit steam cooling system for nozzle and rotor blades (CCSCN-R) in efficiency by reducing the consumption of cooling steam and an efficiency of 60 HHV% was achievable.

The water cooled first-stage nozzle blade and the steam cooled first-stage rotor blade for the CCWCN-SCR were designed. The nozzle blade had a copper alloy for its core to reduce thermal stress and advanced coating technologies were used to protect its core material. The combination of CZ-Cu and a thermal barrier coating (TBC) was chosen with respect to its high thermal barrier effect. The multihole cooling design was found feasible for such high thermal-load conditions. However, as regards toughness and durability for other applications, combination of the copper alloy and a metal coating is also conceivable.

The rotor blade used a conventional nickel-base single crystal

alloy with a TBC. The intensified internal serpentine cooling with V-shaped staggered turbulence promoter ribs also was found capable, only allowing film cooling at the leading edge part.

Present blade cooling depends on coating technologies, therefore reliable and durable coatings that can be operated under higher thermal load conditions are required.

The authors have designed the water cooled nozzle test blade and the steam cooled rotor test blade, which were 50% scale models, based on the concepts described in this paper and are planning to test them to verify their design validity under an actual temperature by using hydrogen-fueled combustor this year.

ACNOWLEDGEMENTS

REFERENCES

Alderson, E. D., Scheper, G. W., and Cohn, A., 1987, "Closed Circuit Steam Cooling in Gas Turbines", ASME paper, 87-JPGC-GT-1.

Anzai, S., Kawaike, K., Matsuzaki, H., and Takehara, I., 1991, "Effect of Turbulence Promoter Rib Shape on Heat Transfer and Pressure Loss Characteristics," J. of the Gas Turbine Society of Japan, Vol. 20, No. 75, pp.65-73 (in Japanese).

Geiling, D.W., Klompas, N., and Zeman, K.P., 1983, "Water Cooled Gas Turbine Nozzle Technology Demonstration at Ultra-High Firing Temperature," ASME Paper, 83-GT15.

Han, J.C., Park, J.S., and Lei, C.K., 1985, "Heat Transfer Enhancement in Channels with Turbulence Promoters," ASME J. of Engineering for Gas Turbine and Powers, Vol.107, pp.629-635.

Ikeguchi, T. and Kawaike, K., 1994, "Effect of Closed-Circuit Gas Turbine Cooling Systems on Combined Cycle Performance," ASME Paper, 94-JPGC-GT-8.

Jericha, H., Starzer, O., and Theissing, M., 1991, " Towards a Solar-Hydrogen System," ASME Cogen-Turbo, IGTI-Vol.6, pp.435-442.

Kawaike, K., Kobayashi, N., and Ikeguchi, T, 1984, "Effects of New Blade Cooling System with minimized Gas Temperature Dilution on Gas Turbine Performance," Trans. of ASME, J. of Engineering for Gas Turbine and Power.

Kawaike, K., Anzai, S., and Sasada, T., 1992, "Integrated CAE System for Cooled Turbine Blade Design and Verification Tests of Analytical Codes," Heat Transfer in Turbomachinery, Goldstein, R. J. et al., ed., Begell House, Inc., pp.73-84 Proceedings of International Symposium Heat Transfer in Turbomachinery, International Center for Heat and Mass Transfer.

Kawaike, K. Anzai, S., Takehara, I., Sasada, T., and Matsuzaki, H., 1993, "Advanced Cooling Design of Turbine Blades with Serpentine Cooling Passages," CIMAC, G12.

Kukreja, R.T., Lau, S.C., and Mcmillin, R.D., 1991, "Effects of Length and Configuration of Transverse Discrete Ribs on Heat Transfer and Friction for Turbulent Flow in a Square Channel," ASME/JSME Thermal Engineering Proceeding, Vol.3, pp.213-218.

Taslim, M.E., Li, T., and Kercher, D.M., 1994, "Experimental Heat Transfer and Friction in Channels Roughened with Angled, V-shaped and Discrete Ribs on Two Opposite Walls," ASME Paper. 94-GT-163.